



Development of laminated nanocomposites on the bases of magnetic and non-magnetic shape memory alloys: Towards new tools for nanotechnology



Artemy Irzhak^a, Viktor Koledov^b, Dmitry Zakharov^{a,*}, Gor Lebedev^a, Alexey Mashirov^b, Veronika Afonina^b, Kristina Akatyeva^b, Vladimir Kalashnikov^b, Nikolay Sitnikov^c, Natalia Tabachkova^a, Alexander Shelyakov^c, Vladimir Shavrov^b

^a National University of Science and Technology "MISIS", Moscow, Russia

^b Kotelnikov Institute of Radioengineering and Electronics of the Russian Academy of Sciences, Moscow, Russia

^c National Research Nuclear University "MEPhI", Moscow, Russia

ARTICLE INFO

Article history:

Available online 2 November 2012

Keywords:

Shape memory alloy
Nanocomposite
Ti–Ni–Cu
Ni–Mn–Ga

ABSTRACT

New composite functional material with shape memory effect (SME) has recently been proposed and tested for actuation on microscale. The composite nanotweezers have been designed and tested in manipulation of nano-objects. This report presents the new experiments on shape memory alloy's (SMAs) properties on submicron scale of dimensions and the development of the technology of nanomanipulation on their bases. The minimal thickness of shape memory layer that undergoes SME was experimentally estimated for Ti₂NiCu alloy. Impact of the focused ion beam modification of SMA superficial layer on the shape memory properties of micro-sized samples is discussed. Composite actuator of Ni–Mn–Ga magnetic SMA with the size of $20 \times 4 \times 2 \mu\text{m}^3$ was fabricated for the first time and its thermal actuation was experimentally demonstrated (<http://www.smwsm.org/microactuators/NiMnGa.html>).

© 2012 Elsevier B.V. All rights reserved.

1. Introduction

Recently, much effort was made on designing of new functional composites on the base of amorphous and nanostructured materials with maximal controllable strain. The new composite functional material with shape memory effect (SME) has been proposed and proved to have up to several percent of thermally controllable strain [1–5]. The prototype of the nanotweezers has been developed and applied for 3D manipulation of carbon nanotubes (CNTs), nano-whiskers, biological micro-objects, etc. [6–9]. The present report is devoted to the new experiments on shape memory alloy's (SMAs) properties on submicron scale and the fundamentals of the development of the new technology of nanomanipulation on their bases.

We discuss: (1) the experiments on the preparation of composite microactuators based on Ti₂NiCu SMA layers with different thicknesses by focused ion beam (FIB) milling and tests of their thermal actuation properties with a purpose to estimate the lowest boundary of SME manifestation; (2) the characterization using transmission electron microscopy (TEM) for studying the surface structure of the micro-samples of the Ti₂NiCu alloy processed by

FIB in order to separate the impacts of technological restriction on the minimal functional layer thickness and of fundamental limitation of thermoelastic martensitic transition and SME manifestation on nanoscale; (3) the experiments on preparation and tests of the composite microactuators from ferromagnetic SMA Ni–Mn–Ga which are directed to the development of the new technology of bio-micromechanical devices actuated at constant temperature by magnetic field.

2. Shape memory actuation on submicron scale

2.1. State of the art

Shape memory actuation on submicron scale is still a difficult task since the manifestation of SME, the transition temperatures and generated strain are very sensitive to numerous parameters which are hard to control in micro-samples: mechanical stresses, microstructure, superficial layer state, etc. [9,10]. Besides, there exists a physical limitation on the size of the SMA sample which undergoes thermoelastic martensitic transformation and associated SME [11,12]. Whereas 105 nm thin NiTi SMA sample was shown to exhibit thermoelastic martensitic transformation [13], the direct demonstration of shape recovery was made only for 200 nm sample [11].

* Corresponding author. Tel.: +7 495 629 3506.

E-mail address: dmitry.zakharov@mis.ru (D. Zakharov).

In our previous work we have made an upper experimental estimate of the critical thickness for Ti_2NiCu SMA at 140 nm [8]. Here we give a lower estimate and discuss the physical and technological contributions in the size limitation for the case of FIB milling.

2.2. The smallest bimorph actuators based on Ti_2NiCu SMA

Forty micrometre thick melt spun ribbons of rapidly quenched alloy $\text{Ti}_{50}\text{Ni}_{25}\text{Cu}_{25}$ with SME taking place at the temperature range from 40 °C to 60 °C were used. The fabrication of the ribbons and their preliminary preparation method were described in [7]. Bilayered composite cantilevers were fabricated by FIB milling followed by ion-assisted deposition of Pt elastic layer from an organometallic gas precursor. The details of the fabrication technology and the platinum layer properties were discussed in [8]. Shape memory actuation was realized by heating the cantilevers with the laser radiation.

The smallest working actuator fabricated by our group had the dimensions of $3 \times 1 \times 0.3 \mu\text{m}^3$. Its SMA layer was 140 nm, and the reversible bending on thermocycling was clearly observed (Fig. 1a and b). It was calculated in [8] that the bending deformation of this actuator was about 0.8%. The smaller actuators with the thickness of SMA layer down to 70 nm have demonstrated progressive deterioration of the actuation. For two actuators with the thickness of SMA of 70 nm no visible deformation on thermocycling was observed (Fig. 1c and d). So we can infer from these experiments the estimation for lower limit of the smallest thickness of the active layer of the Ti_2NiCu alloy with SME processed by FIB demonstrating effective actuation is between 170 nm and 70 nm. The question arises about the origin of this limit. Both fundamental and technological reasons can give rise to the limitation of SME manifestation.

2.3. Shape memory composite actuator as a microinstrument

The proposed shape memory composite actuator can be applied in designing various micro-mechanical systems. For example, micro-sized tweezers and clips for manipulation of submicron- and nano-sized objects can be developed. Such instruments of various sizes based on other physical effects (such as thermal expansion, electrostatic attraction, etc.) have recently been proposed [14–17]. However, micromechanical instruments based on SME would have a smaller size thanks to stronger deformation and stronger force generated by SMA. This could allow one developing the

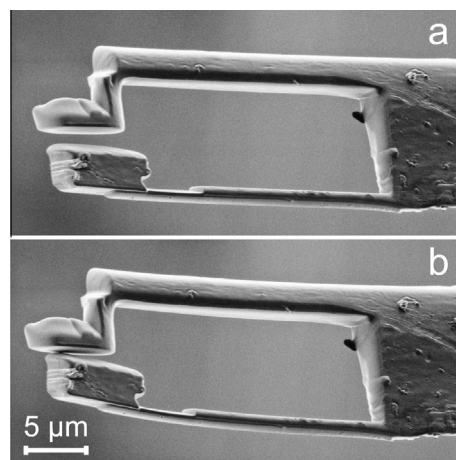


Fig. 2. Microimage of the micro-sized nanotweezers based on the composite with SME. (a) At cold (martensite) state, (b) at hot (austenite) state. The lower part of the nanotweezers is a bimorph cantilever $\text{Ti}_2\text{NiCu}/\text{Pt}$ which bends on heating.

manipulation tools with the sizes close to that of the manipulated objects.

Fig. 2 shows the shape memory nanotweezers attached to the tip of the standard half grid TEM sample holder. The upper part of the nanotweezers is a bimorph cantilever with SME which bending deformation is thermally controlled [8]. Nanotweezers designed in this way can hold a nano-object on heating (see video at [18,19]). Obviously, by placing the passive part of the tweezers from the other side, they could be designed to be closed at cold state. Such a microinstrument could be used as a micro-sized nano-clip. Developing of the technology for nano-clip fabrication is now in progress.

3. Technological limitation on the size of shape memory actuators prepared by FIB milling

The FIB milling leads to the damage of the surface of SMA. The result is the formation of an amorphous passive layer on the surface of the sample. The study by TEM of the surface structure of the Ti_2NiCu samples produced by FIB milling has been undertaken in order to estimate the technological restrictions on the minimal thickness of the active layer of the actuator.

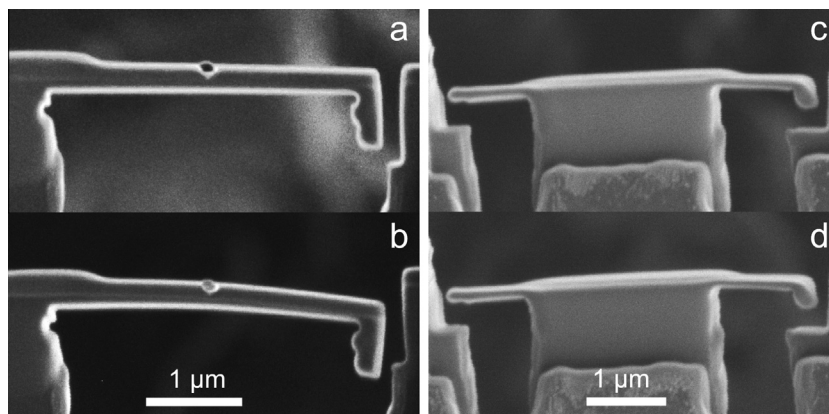


Fig. 1. FIB secondary electron images of the smallest composite cantilevers on the base of SMA fabricated in this work. (a and b) Ti_2NiCu (140 nm)/Pt (160 nm) nanocomposite at cold (martensite) and hot (austenite) state, respectively. (c and d) Ti_2NiCu (70 nm)/Pt (70 nm) nanocomposite at cold (martensite) and hot (austenite) state, respectively.

3.1. Experimental procedure

The ribbon of the Ti_2NiCu alloy has been prepared as described above. In order to study the structure of the surface of the alloy sample processed by FIB, a sample for TEM was prepared as follows.

1. Homogeneous flat area was chosen on the ribbon surface and placed perpendicularly to the ion beam.
2. Squares of 2×2 and $5 \times 5 \mu\text{m}^2$ were exposed to various ion currents (from 150 nA to 1000 nA) and various energies of the gallium ions (from 20 keV to 30 keV) to mill a crater with the depth of 2 μm . In this way a damaged material is formed on bottom and walls of the crater.
3. Thin protective metal layers with total thickness of about 60 nm were deposited by conventional magnetron sputtering. This provides non destructive covering of the amorphous layer.
4. Additional 0.5 μm thick protective layer of organometallic compound of Pt and C was deposited by FIB-CVD.
5. TEM lamella was then cut off by a standard lift-out technique [20] and attached to TEM grid. In this way, the damaged material on the bottom of the crater was prepared for study.

3.2. TEM studies results

The examples of TEM microphotography and microdiffraction pattern are presented in Fig. 3. The amorphous layer with clear boundary is observed on the surface of the ion beam treated samples. The thicknesses of the amorphous layers in different regions were varied from 18 nm to 35 nm depending on the energy of Ga ions. The amorphous layer depth is almost independent on the ion current. Its structure is proved to be amorphous by studying microdiffraction pattern, which is shown in the inset of the Fig. 3.

This direct observation of the passive amorphous layer with clearly measured depth near 30 nm explains hindering of SME in the active alloy layers thinner than 100 nm. More detailed study should clarify fundamental limitation on martensitic structure and SME manifestation. New nanotechnological approaches may

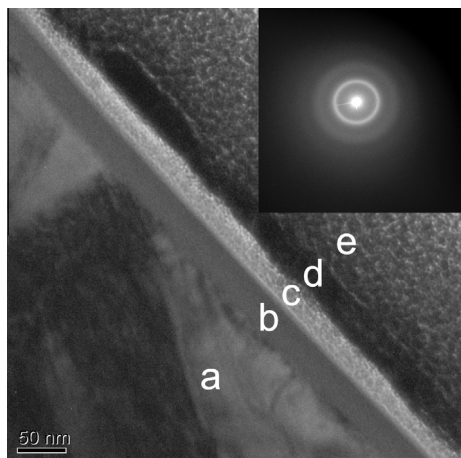


Fig. 3. Bright-field TEM image of the surface of the Ti_2NiCu alloy processed by FIB. (a) – layer of the Ti_2NiCu in crystalline state; (b) – amorphous layer of Ti_2NiCu alloy; (c and d) protective metal layers; (e) Pt–C organometallic protective layer. The inset: microdiffraction of the amorphous Ti_2NiCu layer.

help to create submicron-sized microinstruments with active layer thicknesses below 100 nm.

4. Microactuators on the base of magnetic SMAs

Since the demonstration of the magnetic control of SME at constant temperature in polycrystalline $\text{Ni}_2\text{MnGa(Fe)}$ Heusler alloy [21], much efforts have been directed to the development of practical actuators on its base. In the present work, the composite microactuators on the base of Ni–Mn–Ga melts spun ribbon have been prepared and heat controlled actuation was tested.

4.1. Preparation of composite actuator on the base of Ni–Mn–Ga ferromagnetic SMA

The melt-spun ribbons with the nominal composition $\text{Ni}_{53}\text{Mn}_{24}\text{Ga}_{23}$ of 30 μm -thickness have been prepared by melt spinning. Some pieces of ribbons were annealed in vacuum at 800 $^{\circ}\text{C}$ for 72 h. At room temperature all samples were in ferromagnetic and martensitic state. Their Curie point (T_C) as well as their start and finish temperatures of austenite–martensite and martensite–austenite transformations (M_s , M_f , A_s and A_f , respectively) were determined by differential scanning calorimetry (DSC). For the sample annealed for 72 h, $M_s = 49.5$, $M_f = 41.2$, $A_s = 50.4$, $A_f = 60.7$, and $T_C = 72.5$ $^{\circ}\text{C}$. More details on the preparation and other parameters of the ribbons are given elsewhere [22–24]. Previously, we have shown a technology for generating a pronounced two-way SME for micro-sample of this alloy [25].

The cantilever-type composite actuator Ni–Mn–Ga/Pt with the dimensions of $20 \times 4 \times 2 \mu\text{m}^3$ has been prepared by FIB milling. Up to our knowledge, this is the smallest Ni–Mn–Ga-based actuator made to date. The steps of the preparation procedure are illustrated by Fig. 4. The platinum elastic layer was applied on Ni–Mn–Ga alloy surface by FIB-CVD as described above (Fig. 4a). Then, the rectangular actuator body was cut by FIB milling. This process is shown in Fig. 4b, with martensitic twins of Ni–Mn–Ga alloy being clearly visible on scanning ion beam microscopic image. On the last stage of the preparation procedure, the ferromagnetic Ni–Mn–Ga/Pt composite with SME was attached by FIB-CVD to the tip of the needle of OmniProbe[®] nanomanipulator and moved to silicon substrate and attached thereon (Fig. 5).

4.2. Experiments on thermal actuation of ferromagnetic shape memory composite

The test of the composite actuator has been performed by thermal actuation using semiconductor laser radiation in vacuum chamber of FIB device as shown on the Fig. 5a and b (see video on the web [26]). The laser was GaAl/GaAlAs heterostructure with a wavelength of 0.9 μm . Flexural deformation of actuator was observed when pump current was from 0.5 A to 0.7 A. At this current, laser optical power was about 100 mW for the spot of 1 mm. Since SME in the initial ribbon took place at about 50 $^{\circ}\text{C}$, it is supposed that microactuator deformation happened at approximately the same temperatures. Time of actuator response was of order of 0.1 s. The analysis of the images obtained by scanning ion microscope gives the value of controllable strain of about 1%. Long term operation of actuators at 1000 of thermocycles without degradation is confirmed.

The magnetic field which should be applied to control the actuator at constant temperature can be estimated, knowing the sensitivity of martensitic transition of the alloy to magnetic field and the thermal hysteresis of martensitic transition. For Ni–Mn–Ga alloy, the sensitivity is near to 1 K/T and thermal hysteresis is of order

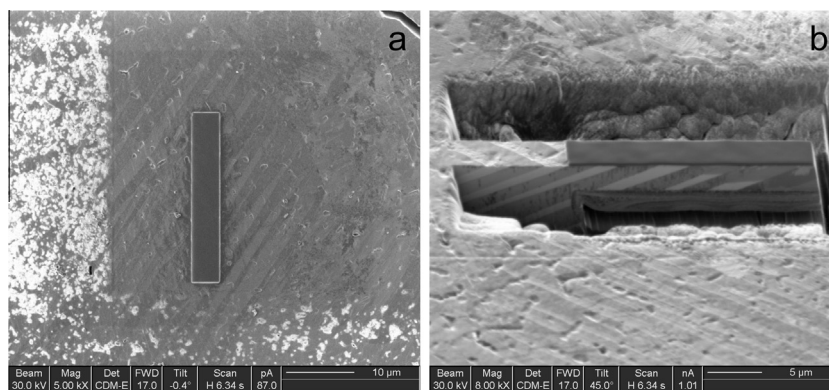


Fig. 4. The fabrication stages of ferromagnetic SMA microactuator. (a) deposition of platinum layer by FIB/CVD on the surface of Ni–Mn–Ga alloy. (b) Preparation of Ni–Mn–Ga/Pt composite microactuator by FIB milling. The structure of martensitic twins on the surface of Ni–Mn–Ga alloys can be clearly observed.

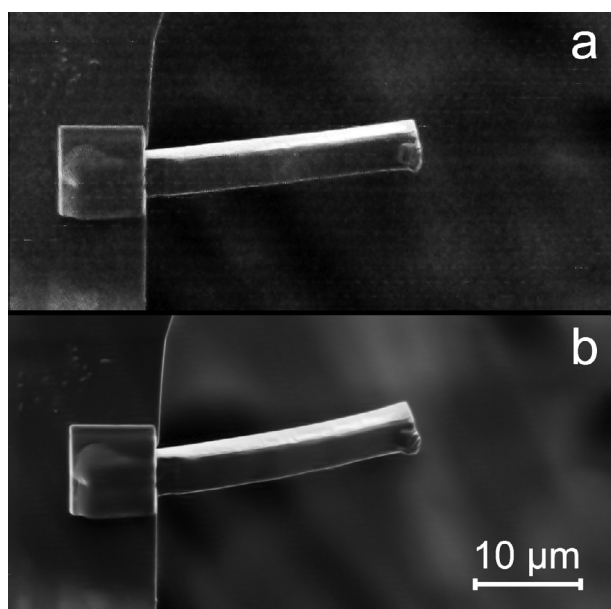


Fig. 5. Microactuator on the base of Ni–Mn–Ga/Pt composite with SME. (a) At cold (martensite) state and (b) at hot (austenite) state. (see video on the web: [25]).

of 10 K, which gives about 10 T magnetic field [21]. Recently, new ferromagnetic Heusler alloys with SME were discovered (NiMnIn, NiMnInCo) with the sensitivity of martensitic transition to magnetic field of up to 10 K/T [27]. In principal, application of these new Heusler alloys can make possible the control of microinstruments by a field of cheap and robust permanent magnets (2 T and less).

5. Conclusions

We may say in conclusion that recent studies on the micro- and nanocomposite actuators with SME prepared by FIB milling allow to estimate the lowest limit of active layer thickness of SME manifestation between 170 nm and 70 nm. Prototype of the working actuator has been fabricated with the overall size of about $1 \mu\text{m}^3$.

TEM experiments revealed 25 nm–35 nm amorphous layer on the surface of T_2NiCu SMA processed by FIB. This can lead to technological restrictions of the lowest thickness of active layer of microactuators. Further studies, both technological and physical, should separate physical and technological impacts to the limit

of lowest active layer thickness and minimal size of microinstruments with SME. The proper accounting for these impacts can open the possibility to design effective microinstruments with overall size less than $1 \mu\text{m}^3$.

Wide variety of applications, especially in the field of micro-biomanipulation, could be opened using nano and microinstruments on the bases of magnetic SMAs. Shape memory composite on the base of ferromagnetic Ni–Mn–Ga SMA was fabricated for the first time and its thermal actuation was demonstrated in vacuum chamber of FIB device. Up to our knowledge, to date it is the smallest actuator made of this alloy. Novel magnetic SMAs with higher sensitivity of martensitic transition to magnetic field should be applied to develop a technology for practical microinstruments working at constant temperature. Such microinstruments might help to resolve some unresolved problems of medicine and biotechnology, particularly in single cell manipulation, microsurgery, drug delivery systems, etc.

Acknowledgements

Authors are grateful to professors V. Pushin, S. Belyaev, P. Ari-Gur and F. Albertini for discussions. The authors also thank N. Pikhtin and I. Tarasov for development and fabrication of the laser.

The research was carried out with the financial support of the Programme of Creation and Development of the National University of Science and Technology ‘MISiS’.

The research was financially supported by the Ministry of Education and Science of the Russian Federation (G.K. 16.552.11.7009), RFBR (Grants No. 11-02-90502, 11-08-92504, 12-07-00811), RAS-CNR Joint Research Program, and by the PRRIITT Program of the Emilia-Romagna Region in the frame of the MIST E-R Laboratory. Investigations were carried out using the equipment of Common-Use Scientific Center ‘Material Science and Metallurgy’ at NUST ‘MISiS’ and the equipment of CKP MIPT and REC ‘Nanotechnology’ at Moscow Institute of Physics and Technology.

References

- [1] D.I. Zakharov, A.G. Kirilin, V.V. Koledov, G.A. Lebedev, E.P. Perov, V.G. Pushin, V.V. Khovailo, V.G. Shavrov, A.V. Shelyakov, *Funct. Mater.* 15 (3) (2008) 448–454.
- [2] V. Khovaylo, G. Lebedev, D. Zakharov, V. Koledov, E. Perov, V. Shavrov, M. Ohtsuka, V. Pushin, H. Miki, T. Takagi, *Jpn. J. Appl. Phys.* 49 (2010) 100212.
- [3] A.V. Irzhak, V.S. Kalashnikov, V.V. Koledov, D.S. Kuchin, G.A. Lebedev, P.V. Lega, N.A. Pikhtin, I.S. Tarasov, V.G. Shavrov, A.V. Shelyakov, *Tech. Phys. Lett.* 36 (4) (2010) 329–332.
- [4] D. Zakharov, G. Lebedev, V. Koledov, P. Lega, D. Kuchin, A. Irzhak, V. Afonina, E. Perov, A. Shelyakov, V. Pushin, V. Shavrov, *Phys. Procedia* 10 (2010) 58–64.
- [5] A.V. Irzhak, D.I. Zakharov, V.S. Kalashnikov, V.V. Koledov, D.S. Kuchin, G.A. Lebedev, P.V. Lega, E.P. Perov, N.A. Pikhtin, V.G. Pushin, I.S. Tarasov, V.V.

- Khovailo, V.G. Shavrov, A.V. Shelyakov, J. Commun. Technol. El. 55 (7) (2010) 818–830.
- [6] A. Shelyakov, N. Sitnikov, V. Koledov, D.S. Kuchin, A.V. Irzhak, N.Yu. Tabachkova, Int. J. Smart Nano Mater. 2 (2) (2011) 68–77.
- [7] A.V. Shelyakov, N.N. Sitnikov, A.P. Menushenkov, V.V. Koledov, A.I. Irzhak, Thin Solid Films 519 (2011) 5314–5317.
- [8] D. Zakharov, G. Lebedev, A. Irzhak, V. Afonina, A. Mashirov, V. Kalashnikov, V. Koledov, A. Shelyakov, D. Podgorny, N. Tabachkova, V. Shavrov, Smart Mater. Struct. 21 (2012) 52001.
- [9] S. Miyazaki, Y. Fu, W. Huang, Thin Film Shape Memory Alloys: Fundamentals and Device Applications, Cambridge University Press, Cambridge, 2009.
- [10] J. Ye, R.K. Mishra, A.R. Pelton, A.M. Minor, Acta Mater. 58 (2010) 490–498.
- [11] J.M. San Juan, M.L. No, C.A. Schuh, Adv. Mater. 20 (2008) 272–278.
- [12] Y.-Q. Fu, S. Zhang, M.J. Wu, W.M. Huang, H.J. Du, J.K. Luo, A.J. Flewitt, W.I. Milne, Thin Solid Films 515 (1) (2006) 80–86.
- [13] B.G. Clark, D.S. Gianola, O. Kraft, C.P. Frick, Adv. Eng. Mater. 12 (8) (2010) 808–815.
- [14] A. Cagliani, R. Wierzbicki, L. Occhipinti, D.H. Petersen, K.N. Dyvelkov, O.S. Sukas, B.G. Herstrom, T. Booth, P. Boggild, J. Micromech. Microeng. 20 (2010) 035009.
- [15] K.J. Briston, A.G. Cullis, B.J. Inkson, J. Micromech. Microeng. 20 (2010) 015028.
- [16] J. Chang, B.-K. Min, J. Kim, S.-J. Lee, L. Lin, Smart Mater. Struct. 18 (2009) 065017.
- [17] M. Kumemura, D. Collard, N. Sakaki, C. Yamahata, M. Hosogi, G. Hashiguchi, H. Fujita, J. Micromech. Microeng. 21 (2011) 054020.
- [18] <<http://www.smwsm.org/ll/micropincer.html>>.
- [19] <<http://www.smwsm.org/microactuators/nanotweezers.html>>.
- [20] L.A. Giannuzzi, F.A. Stevie, Introduction to Focused Ion Beams: Instrumentation, Theory, Techniques, and Practice, Springer, New York, 2005.
- [21] A.A. Cherechukin, I.E. Dikshtein, D.T. Ermakov, A.V. Glebov, V.V. Koledov, D.A. Kosolapov, V.G. Shavrov, A.A. Tulaikova, E.P. Krasnoperov, T. Takagi, Phys. Lett. A 291 (2–3) (2001) 175–183.
- [22] F. Albertini, S. Besseghini, A. Paoluzi, L. Pareti, M. Pasquale, F. Passaretti, C.P. Sasso, A. Stantero, E. Villa, J. Magn. Magn. Mater. 242 (2002) 1421–1424.
- [23] F. Albertini, S. Besseghini, A.S. Bugaev, R.M. Grechishkin, V.V. Koledov, L. Pareti, M. Pasquale, V.G. Shavrov, D.S. Yulenkov, J. Commun. Technol. El. 50 (2005) 638–646.
- [24] F. Albertini, F. Algarabel, P.A. Magen, L. Morellón, M.R. Ibarra, F. Albertini, N. Magnani, A. Paoluzi, L. Pareti, M. Pasquale, S. Besseghini, J. Magn. Magn. Mater. 272–276 (2004) 2047–2048.
- [25] K. Akatyeva, V. Afonina, F. Albertini, S. von Gratoski, A. Irzhak, S. Fabbri, V. Khovaylo, V.V. Koledov, E. Krasnoperov, V.G. Shavrov, Solid State Phenomena 190 (2012) 295–298.
- [26] <<http://www.smwsm.org/microactuators/NiMnGa.html>>.
- [27] R. Kainuma, Y. Imano, W. Ito, Y. Sutou, H. Morito, S. Okamoto, O. Kitakami, K. Oikawa, A. Fujita, Nature 439 (2006) 957–960.